AD-A072 199 ARMY MATERIALS AND MECHANICS RESEARCH CENTER WATERTOWN MA F/G 20/11
ILLUSTRATIONS OF TWO SIMPLE METHODS OF DETERMINING STRESS INTEN--ETC(U)
APR 79 F I BARATTA

UNCLASSIFIED AMMRC-MS-79-3 NL

| OF |
AD
A072199

END
DATE
FILMED
9-79
DDC

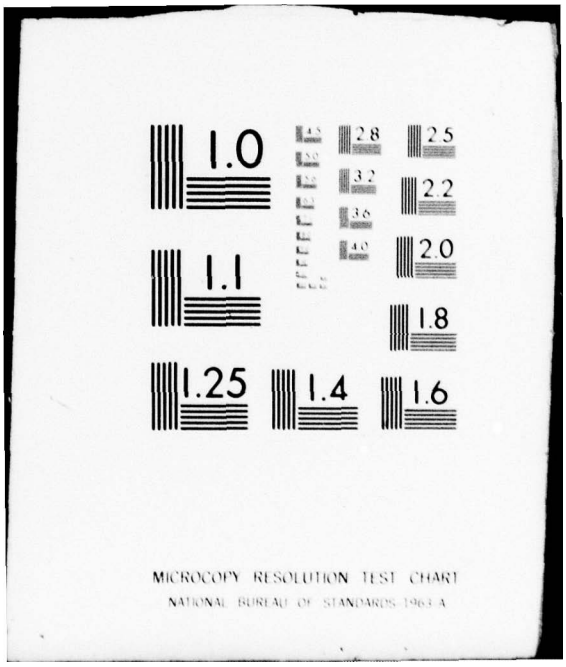
1.0
1.1
1.25
1.4
1.6
1.8
2.0
2.2
2.5
2.8
3.2
3.6
4.0
MICROCOPY RESOLUTION TEST CHART
NATIONAL BUREAU OF STANDARDS 1963-A

AMMRC MS 79-3

LEVEL II

AD

ILLUSTRATIONS OF TWO SIMPLE METHODS OF DETERMINING STRESS INTENSITY FACTORS FROM: (a) STRESS CONCENTRATIONS AND (b) STRESS DISTRIBUTIONS

April 1979

Approved for public release; distribution unlimited.

ARMY MATERIALS AND MECHANICS RESEARCH CENTER
Watertown, Massachusetts 02172

The findings in this report are not to be construed as an official Department of the Army position, unless so designated by other authorized documents.

Mention of any trade names or manufacturers in this report shall not be construed as advertising nor as an official indorsement or approval of such products or companies by the United States Government.

DISPOSITION INSTRUCTIONS

Destroy this report when it is no longer needed.
Do not return it to the originator.

UNCLASSIFIED

SECURITY CLASSIFICATION OF THIS PAGE (When Data Entered)

REPORT DOCUMENTATION PAGE	READ INSTRUCTIONS BEFORE COMPLETING FORM
1. REPORT NUMBER: AMMRC-MS-79-3 (14) (6)	2. GOVT ACCESSION NO.
3. RECIPIENT'S CATALOG NUMBER	
4. TITLE (and Subtitle): ILLUSTRATIONS OF TWO SIMPLE METHODS OF DETERMINING STRESS INTENSITY FACTORS FROM: (a) STRESS CONCENTRATIONS AND (b) STRESS DISTRIBUTIONS	5. TYPE OF REPORT & PERIOD COVERED: (9) Final Report, (6)
	6. PERFORMING ORG. REPORT NUMBER
7. AUTHOR(s): (10) Francis I. Baratta	8. CONTRACT OR GRANT NUMBER(s)
9. PERFORMING ORGANIZATION NAME AND ADDRESS: Army Materials and Mechanics Research Center, Watertown, Massachusetts 02172, DRXMR-TM	10. PROGRAM ELEMENT, PROJECT, TASK AREA & WORK UNIT NUMBERS: D/A Project: AMCMS Code: 728012.13
11. CONTROLLING OFFICE NAME AND ADDRESS: U. S. Army Materiel Development and Readiness Command, Alexandria, Virginia 22333	12. REPORT DATE: (11) April 1979
	13. NUMBER OF PAGES: 20
14. MONITORING AGENCY NAME & ADDRESS (if different from Controlling Office): (12) 22p.	15. SECURITY CLASS. (of this report): Unclassified
	15a. DECLASSIFICATION/DOWNGRADING SCHEDULE

16. DISTRIBUTION STATEMENT (of this Report)

Approved for public release; distribution unlimited.

17. DISTRIBUTION STATEMENT (of the abstract entered in Block 20, if different from Report)

18. SUPPLEMENTARY NOTES

19. KEY WORDS (Continue on reverse side if necessary and identify by block number)

Stress intensity
Fracture mechanics

20. ABSTRACT (Continue on reverse side if necessary and identify by block number)

(SEE REVERSE SIDE)

DD FORM 1 JAN 73 1473 EDITION OF 1 NOV 65 IS OBSOLETE

UNCLASSIFIED 403 105 pmt

SECURITY CLASSIFICATION OF THIS PAGE (When Data Entered)

Block No. 20

ABSTRACT

Illustrative examples of two methods of determining approximate stress intensity factors from (a) stress concentration factors and (b) from stress distributions are presented.

In the first case several example problems are presented whereby stress intensity factors are obtained from known stress concentration factor data. These illustrative problems include data obtained from both closed form and experimental solutions. The results of this method are compared to a well-known, accurate analysis, and guidelines regarding such usage are presented.

In the second case several approximate methods of determining stress intensity factors utilizing stress distributions available in the literature are presented to the reader. Example problems are illustrated and compared to more accurate results when available. Estimates of the accuracy and limited guidance on the usage of such methods are given.

FOREWORD

The two illustrative methods of determining stress intensity factors described herein were previously written as part of a chapter to be included in an AGARDagraph report entitled "On Practical Applications of Fracture Mechanics." Since these two methods are of interest to the technical community it was considered worthwhile to publish them as a monograph.

It is also intended that the results summarized in the present document will become part of a more complete standardization type handbook that will provide easy access to stress intensity factors directly related to Army applications.

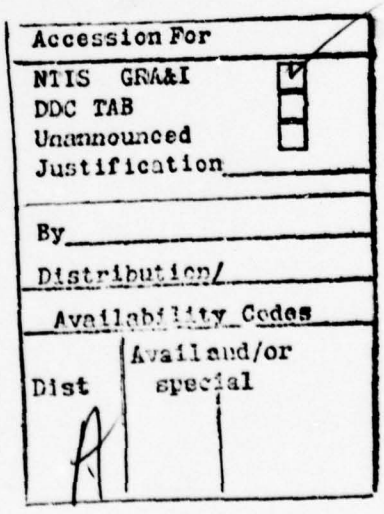

CONTENTS

PART A. STRESS INTENSITY FACTORS FROM STRESS CONCENTRATIONS

INTRODUCTION

Stress intensity factors K may be computed from stress concentration factors as the notch radius ρ approaches zero. This may be observed by noting that a crack with a small but finite tip radius ρ still has its tip embedded within the stress field as described by the elastic stress field equations for mode I given below[1] as the crack tip is approached, i.e., as $r \to 0$:

$$\sigma_{xx} = \frac{K_I}{\sqrt{2\pi r}} \cos\frac{\theta}{2}\left(1-\sin\frac{\theta}{2}\sin\frac{3\theta}{2}\right),$$

$$\sigma_{yy} = \frac{K_I}{\sqrt{2\pi r}} \cos\frac{\theta}{2}\left(1+\sin\frac{\theta}{2}\sin\frac{3\theta}{2}\right), \text{ and} \qquad (1)$$

$$\tau_{xy} = \frac{K_I}{\sqrt{2\pi r}} \sin\frac{\theta}{2}\cos\frac{\theta}{2}\cos\frac{3\theta}{2}.$$

Of course, very near the tip itself, the finite radius will alter the stress distribution. However, the maximum stress σ_{max} will occur on the notch and must be proportional in intensity to the stress field around it, i.e.:

$$\sigma_{max} \propto K_I. \qquad (2)$$

The only characteristic dimension available to make Equation 2 complete is the notch radius ρ, consequently

$$K_I = Q\sigma_{max}\,\rho^{\frac{1}{2}} \qquad (3)$$

where Q is a numerical constant.

For an elliptical hole stressed by σ_0 in an infinite sheet, the stress concentration equation[2] is:

$$\frac{\sigma_{max}}{\sigma_0} = \left[1+2(c/\rho)^{\frac{1}{2}}\right], \qquad (4)$$

where 2c is the major axis of the ellipse.

The stress intensity equation for a through crack of length 2a which the ellipse degenerates to in the limit is:

$$K_I = \sigma_0\,(\pi a)^{\frac{1}{2}}. \qquad (5)$$

1. PARIS, P. C., and SIH, G. C. *Stress Analysis of Cracks.* ASTM Special Technical Publication 381, 1970, p. 30-80

2. ENGLIS, C. E. *Stresses in a Plate Due to the Presence of Cracks and Sharp Corners.* Trans. Instn. Nav. Archit., v. 55, 1913, p. 219.

Substitution of Equations 4 and 5 into Equation 3 and taking the limit as $\rho \to 0$, gives $Q = \frac{\pi^{\frac{1}{2}}}{2}$, as indicated in the following:

$$\sigma_0(\pi a)^{\frac{1}{2}} = Q\,\sigma_0[1+2(c/\rho)^{\frac{1}{2}}]\,\rho^{\frac{1}{2}} \text{ or } Q = \frac{(\pi c)^{\frac{1}{2}}}{\rho^{\frac{1}{2}}+2c^{\frac{1}{2}}} = \frac{\pi^{\frac{1}{2}}}{2}$$

and therefore Equation 3 becomes, as deduced by Erwin:[3]

$$K_I = \lim_{\rho \to 0} \frac{\sqrt{\pi}}{2} k_{t_I} \sigma_0 \rho^{\frac{1}{2}}, \tag{6}$$

for mode I only, provided $K_{II} = K_{III} = 0$; and k_t is the stress concentration factor, i.e., $k_{t_I} = \sigma_{max_I}/\sigma_0$.

Formulas corresponding to Equation 6 can be derived[1,2] for K_{II} for K_{III} as well as K_B, which is a special case of mode I, and these are:

$$K_{II} = \lim_{\rho \to 0} \sqrt{\pi}\, k_{t_{II}}\, \tau_0 \rho^{\frac{1}{2}}, \tag{7}$$

provided $K_I = K_{III} = 0$, where $k_{t_{II}}$ is the in-plane shear stress concentration factor, i.e., $k_{t_{II}} \simeq \frac{\tau_{maxII}}{\tau_0}$.

$$K_{III} = \lim_{\rho \to 0} \sqrt{\pi}\, k_{t_{III}}\, \tau_0 \rho^{\frac{1}{2}}, \tag{8}$$

provided $K_I = K_{II} = 0$, where $k_{t_{III}}$ is the out-of-plane shear stress concentration factor, i.e., $k_{t_{III}} = \frac{\tau_{max_{III}}}{\tau_0}$.

Finally,

$$K_B = 1/2((3+\nu)/(1+\nu)) \lim_{\rho \to 0} M_{max} \tag{9}$$

where ν is Poisson's ratio and M_{max} is the maximum bending moment.

3. IRWIN, G. R. *Fracture Mechanics, Structural Mechanics.* Goodier and Hoff, ed., Pergamon Press, Oxford, 1960.

Equations 6 to 9 provide powerful but simple tools to obtain stress intensity factors directly from stress concentration factors, because included in these limit equations are stress concentration factors. Thus, if the stress concentration factor as a function of ρ for a given loading system is known, by taking ρ to the limit in the appropriate equation given above, the stress intensity factor can be obtained.

There are a number of references available, such as Heywood,[4] Neuber,[5] Peterson[6] and others, that provide experimental stress concentration factor data as well as theoretical expressions for many configurations. The data taken from some of these references as well as others will be utilized in the examples to follow.

EXAMPLE PROBLEMS AND APPLICATIONS

To illustrate the approach, consider the semi-elliptical edge notch of depth c as stressed by σ_0 in a semi-infinite sheet shown in Figure 1. The stress concentration factor k from Bowie[7] is given in Table 1. By reworking the data from Reference 7 (third and fourth columns) so that it is dimensionless, and plotting $k\sqrt{\rho/c}$ as a function of ρ/c as shown in Figure 2 (a semi-log plot), we can graphically determine the limit on K_I as $\rho \to 0$. It is seen from the figure that as $\rho \to 0$, $c \to a$, where c is the crack length. The extrapolated value of $K_I/(\sqrt{\pi a}\ \sigma_0/2)$ approaches 2.26 and thus,

$$\frac{K_I}{\sqrt{\pi a}\ \sigma_0} \simeq \frac{2.26}{2} = 1.13.$$

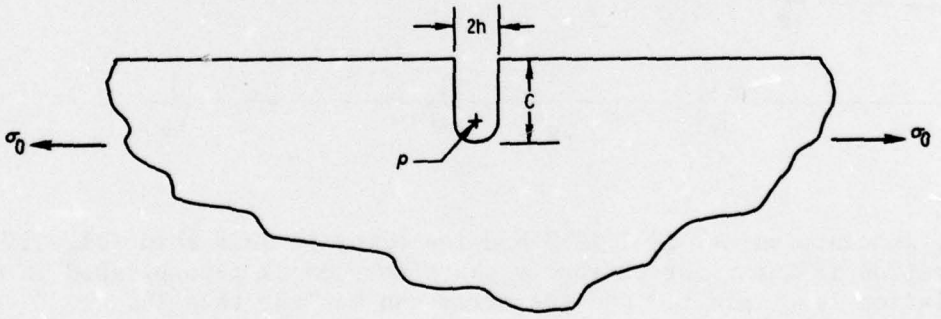

Figure 1. Semi-elliptical edge notch in a semi-infinite sheet.

4. HEYWOOD, R. B. *Designing by Photoelasticity.* London, Chapman, and Hall, Ltd., 1952.
5. NEUBER, H. *Theory of Notch Stress: Principles for Exact Stress Calculation of Strength with Reference to Structural Forms and Materials.* AEC Technical Report, TR No. 4547, 1958.
6. PETERSON, R. E. *Stress Concentration Factors.* John Wiley & Sons, New York, 1974.
7. BOWIE, O. L. *Analysis of Edge Notches in a Semi-Infinite Region.* J. Math. and Physics, v. 45, no. 4, December 1966; also Army Materials and Mechanics Research Center, AMRA TR 66-7, June 1966.

Table 1. REDUCTION OF STRESS CONCENTRATION FACTOR TO STRESS INTENSITY FACTOR

c/ρ	k	ρ/c	$k\sqrt{\rho/c}$
1.0	3.065	1.0	3.065
2.0	3.96	0.50	2.80
3.0	4.63	.333	2.67
4.0	5.20	.25	2.60
6.0	6.16	.167	2.51
9.0	7.41	.111	2.46
16.0	9.625	.063	2.41
32.1	13.320	.031	2.35
81.02	20.77	.012	2.28
361.4	43.2	.0028	2.29

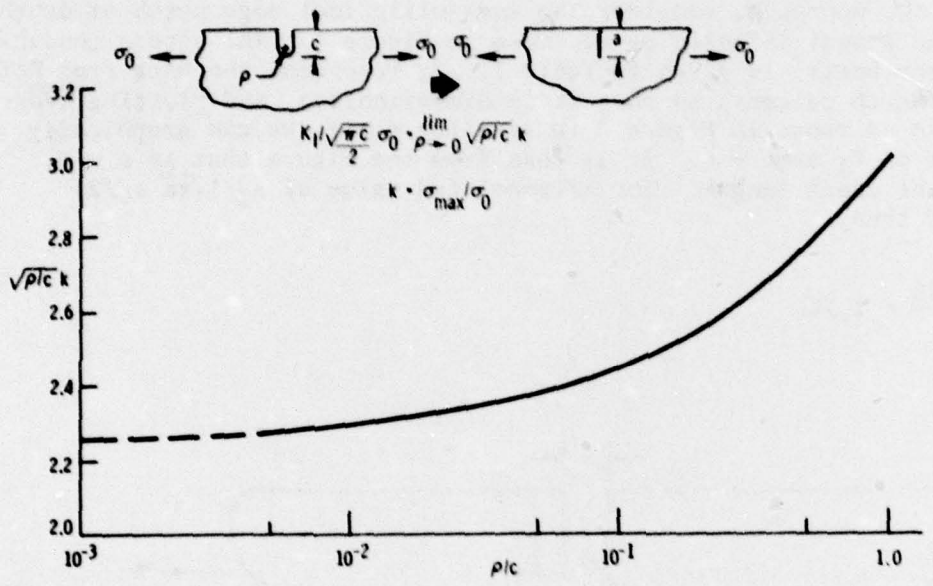

Figure 2. Stress intensity factor from theoretically determined stress concentration factors.

The more accurate value[8] is 1.1215 and the error is less than +1%. If the stress concentration is known for extremely sharp notches as accomplished in Reference 9, extrapolation is eliminated and the error can be less than 1%.

Experimental data can be handled in a similar fashion as that given in the preceding example. Consider the experimental data given by Frocht[10] for relatively deep symmetrical U-notches in a finite plate of notch depth-to-plate width L/b of 1/2. This data is now presented in dimensionless form in Figure 3; $\sqrt{\rho/L}\,k$ is plotted as a function of ρ/L on semi-log paper.

8. KOITER, W. T. *On the Flexural Rigidity of a Beam Weakened by Transverse Saw-Cuts.* J. Appl. Mech., v. 32, 1965, p. 237.
9. HASEBE, N., and KUTANDA, Y. *Calculation of Stress Intensity Factor from Stress Concentration Factor.* Eng. Fracture Mech., v. 10, 1978, p. 215-221.
10. FROCHT, M. M. *A Photoelastic Investigation of Stress Concentrations Due to Small Fillets and Grooves in Tension.* Tech. Notes Nat. Advis. Comm. Aeronaut., Washington, Report No. 2442, 1951.

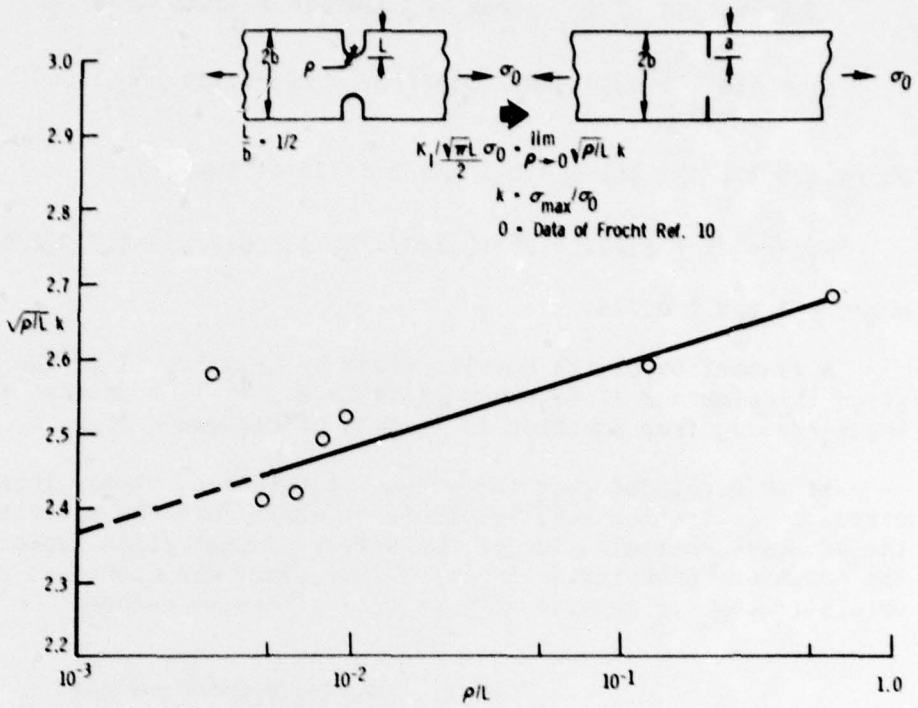

Figure 3. Stress intensity factor from experimental stress concentration data.

Obviously the data point at $\rho/L = 0.030$ is an "outlier"; particularly since the notch acuity is quite sharp, which can result in a large experimental error when attempting to obtain the stress concentration factor by photoelasticity. Therefore, this data point was ignored in Figure 3 and a straight line was drawn through the remaining data resulting in $K/\sigma_0\sqrt{\pi a} = 1.19$ (note as $\rho \to 0$, $L \to a$). The more accurate value is 1.15 from Reference 11 resulting in an error of +3%.

If all of the data in Figure 3 had been utilized to determine K_I by the above extrapolation technique, considerable error would have resulted. By judiciously eliminating the data point(s) that appear to be in error a reasonable approximation to K_I can be realized.

Finally to illustrate how Equation 6 can be applied to a closed-form expression, consider the formula given in Reference 12 which describes the stress concentration factor for symmetrical side-edge U-notches stressed at infinity by σ_0, as shown in Figure 3:

$$k_{t_I} = [0.780+2.243\sqrt{L/\rho}]\,[0.993+0.180(L/b)-1.060(L/b)^2+1.710(L/b)^3] \qquad (10)$$

where $1.0 \leq L/\rho \leq 361$ and $0 \leq L/b \leq 0.723$.

11. BOWIE, O. L. *Rectangular Tensile Sheet with Symmetric Edge Cracks.* Trans. ASME, J. Applied Mech., v. 31, ser. E, no. 2, June 1969.

12. BARATTA, F. I., and NEAL, D. N. *Stress-Concentration Factors in U-Shaped and Semi-Elliptical Shaped Edge Notches.* J. Strain Analysis, v. 5, no. 2, 1970, p. 121-127; also Army Materials and Mechanics Research Center, AMMRC TR 70-1, January 1970.

Substitution of k_{t_I} given by Equation 10 into Equation 6 gives:

$$K_I = \lim_{\rho \to 0} \frac{\pi^{\frac{1}{2}}}{2} \sigma_0 [0.780+2.243\sqrt{L/\rho}] [0.993+0.180\ L/b-1.060(L/b)^2+1.710(L/b)^3] \quad (11)$$

where $1.0 \leq L/\rho \leq 361$ and $0 \leq L/b \leq 0.723$ or finally:

$$K_I/\sqrt{\pi a}\ \sigma_0 = 1.122[0.993+0.180(a/b)-1.060(a/b)^2+1.710(a/b)^3] \quad (12)$$

where $0 \leq L/b \leq 0.723$.

A comparison of the results given by Equation 12 to the more exact data given in Reference 11 is shown in Table 2. It is seen that the error in comparing $K_I/\sqrt{\pi a}\ \sigma_0$ from Equation 12 to that of Reference 11 is no greater than +1%.

It is concluded that the method of obtaining stress intensity factors from stress concentration data is simple to employ but the accuracy is dependent upon the accurate determination of the stress concentration factor as a function of the notch or concentrator acuity. Therefore, the user must provide judgment to obtain reasonable results when utilizing this technique.

Table 2. COMPARISON OF STRESS INTENSITY FACTOR ($K_I/\sqrt{\pi a}\ \sigma_0$) DATA

a/b	From Eq. 12	From Ref. 11	Difference (%)
0.112	1.12	1.12	0
.1667	1.12	1.12	0
.2222	1.12	1.13	0
.3333	1.12	1.13	0
.3889	1.13	1.14	+1
.5001	1.16	1.15	+1
.7230	1.36	1.37	+1

SUMMARY

The method of obtaining K_I from k_{t_I} data is simple and powerful. But accuracy is dependent upon the accurate determination, either experimentally or analytically obtained, of the stress concentration factor as a function of notch acuity. The accuracy of those cases examined was well within that required for engineering applications. However, one should know "a priori" how k_{t_I} generally behaves as a function of notch radius to notch depth and eliminate or include appropriate values for a realistic determination of stress intensity factor at the limit of ρ/c.

Army Materials and Mechanics Research Center,
Watertown, Massachusetts 02172
ILLUSTRATIONS OF TWO SIMPLE METHODS OF DETERMINING STRESS INTENSITY FACTORS FROM: (a) STRESS CONCENTRATIONS AND (b) STRESS DISTRIBUTIONS –
Francis I. Baratta

Monograph Series AMMRC MS 79-3, April 1979, 20 pp – illus-tables, AMCMS Code 728012.13

AD ______________

UNCLASSIFIED
UNLIMITED DISTRIBUTION

Key Words

Stress intensity
Fracture mechanics

Illustrative examples of two methods of determining approximate stress intensity factors from (a) stress concentration factors and (b) from stress distributions are presented. In the first case several example problems are presented whereby stress intensity factors are obtained from known stress concentration factor data. These illustrative problems include data obtained from both closed form and experimental solutions. The results of this method are compared to a well-known, accurate analysis, and guidelines regarding such usage are presented. In the second case several approximate methods of determining stress intensity factors utilizing stress distributions available in the literature are presented to the reader. Example problems are illustrated and compared to more accurate results when available. Estimates of the accuracy and limited guidance on the usage of such methods are given.

Army Materials and Mechanics Research Center,
Watertown, Massachusetts 02172
ILLUSTRATIONS OF TWO SIMPLE METHODS OF DETERMINING STRESS INTENSITY FACTORS FROM: (a) STRESS CONCENTRATIONS AND (b) STRESS DISTRIBUTIONS –
Francis I. Baratta

Monograph Series AMMRC MS 79-3, April 1979, 20 pp – illus-tables, AMCMS Code 728012.13

AD ______________

UNCLASSIFIED
UNLIMITED DISTRIBUTION

Key Words

Stress intensity
Fracture mechanics

Illustrative examples of two methods of determining approximate stress intensity factors from (a) stress concentration factors and (b) from stress distributions are presented. In the first case several example problems are presented whereby stress intensity factors are obtained from known stress concentration factor data. These illustrative problems include data obtained from both closed form and experimental solutions. The results of this method are compared to a well-known, accurate analysis, and guidelines regarding such usage are presented. In the second case several approximate methods of determining stress intensity factors utilizing stress distributions available in the literature are presented to the reader. Example problems are illustrated and compared to more accurate results when available. Estimates of the accuracy and limited guidance on the usage of such methods are given.

Army Materials and Mechanics Research Center,
Watertown, Massachusetts 02172
ILLUSTRATIONS OF TWO SIMPLE METHODS OF DETERMINING STRESS INTENSITY FACTORS FROM: (a) STRESS CONCENTRATIONS AND (b) STRESS DISTRIBUTIONS –
Francis I. Baratta

Monograph Series AMMRC MS 79-3, April 1979, 20 pp – illus-tables, AMCMS Code 728012.13

AD ______________

UNCLASSIFIED
UNLIMITED DISTRIBUTION

Key Words

Stress intensity
Fracture mechanics

Illustrative examples of two methods of determining approximate stress intensity factors from (a) stress concentration factors and (b) from stress distributions are presented. In the first case several example problems are presented whereby stress intensity factors are obtained from known stress concentration factor data. These illustrative problems include data obtained from both closed form and experimental solutions. The results of this method are compared to a well-known, accurate analysis, and guidelines regarding such usage are presented. In the second case several approximate methods of determining stress intensity factors utilizing stress distributions available in the literature are presented to the reader. Example problems are illustrated and compared to more accurate results when available. Estimates of the accuracy and limited guidance on the usage of such methods are given.

Army Materials and Mechanics Research Center,
Watertown, Massachusetts 02172
ILLUSTRATIONS OF TWO SIMPLE METHODS OF DETERMINING STRESS INTENSITY FACTORS FROM: (a) STRESS CONCENTRATIONS AND (b) STRESS DISTRIBUTIONS –
Francis I. Baratta

Monograph Series AMMRC MS 79-3, April 1979, 20 pp – illus-tables, AMCMS Code 728012.13

AD ______________

UNCLASSIFIED
UNLIMITED DISTRIBUTION

Key Words

Stress intensity
Fracture mechanics

Illustrative examples of two methods of determining approximate stress intensity factors from (a) stress concentration factors and (b) from stress distributions are presented. In the first case several example problems are presented whereby stress intensity factors are obtained from known stress concentration factor data. These illustrative problems include data obtained from both closed form and experimental solutions. The results of this method are compared to a well-known, accurate analysis, and guidelines regarding such usage are presented. In the second case several approximate methods of determining stress intensity factors utilizing stress distributions available in the literature are presented to the reader. Example problems are illustrated and compared to more accurate results when available. Estimates of the accuracy and limited guidance on the usage of such methods are given.

PART B. STRESS INTENSITY FACTORS FROM STRESS DISTRIBUTIONS

INTRODUCTION

There are several methods by which stress intensity factors are estimated from stress distributions. For example, Williams and Isherwood[1] approximate the strain energy release rate in terms of a mean stress attributed to the appropriate geometry discontinuity for various problems of interest. Kobayashi[2] applies the stress distribution at the crack face through the use of Green's function in conjunction with the elimination of residual surface tractions which arise because of the geometric discontinuity on the crack surfaces located in the uncracked region. Shah[3] applies a similar procedure but in addition uses the superposition method. Cartwright,[4] rather than applying the stress distribution to the crack face, has estimated stress intensity factors by applying the stress due to the geometry discontinuity to only the crack tip.

These approaches will be demonstrated in the following section by solving several problems and comparing these results to more exact analyses where available. (Cracks inclined to the applied stresses are not considered here.)

METHODS AND APPLICATIONS

Williams and Isherwood[1] determine the strain energy release rate from

$$G = \pi\sigma_m^2 a/E \tag{1}$$

where σ_m is the mean stress, a is the crack length, and E is Young's modulus, by application of the mean stress σ_m over the crack length, assuming no crack is present. This approach can be illustrated by considering Figure 1a, an infinite plate stressed by uniaxial tension σ_0, containing two radial cracks at the boundary of the internal circular hole. The mean stress for this geometric discontinuity is

$$\sigma_m = \int_R^r \frac{\sigma(r)\, dr}{r-R} \tag{2}$$

where from Reference 5 the stress distribution $\sigma(r)$ is:

$$\sigma(r) = \sigma_0[1+(1/2)(R/r)^2+(3/2)(R/r)^4]. \tag{3}$$

1. WILLIAMS, J. G., and ISHERWOOD, D. D. *Calculation of the Strain-Energy Release Rates of Cracked Plates by an Approximate Method.* J. Strain Anal., v. 3, no. 1, 1968, p. 17-22.
2. KOBAYASHI, A. S. *A Simple Procedure for Estimating Stress Intensity Factor in Region of High Stress Gradient.* Significance of Defects in Welded Structures, T. Kanayawa and A. S. Kobayashi, ed., University of Tokyo Press, 1974, p. 127-143.
3. SHAH, R. C. *Stress Intensity Factors for Through and Part-Through Cracks Originating at Fastener Holes.* Mechanics of Crack Growth, J. R. Rice and P. C. Paris, ed., ASTM STP 590, 1976, p. 429-459.
4. CARTWRIGHT, D. J. *Stress Intensity Factors and Residual Static Strength in Certain Structural Elements.* Ph.D. Thesis, Department of Mechanical Engineering, University of Southampton, 1971.
5. TIMOSHENKO, S., and GOODIER, J. N. *Theory of Elasticity.* McGraw-Hill Book Company, Inc., 2nd Edition, 1951.

Substitution of Equation 3 into Equation 2 and integrating between the appropriate limits gives:

$$\sigma_m = \frac{\sigma_0 \left\{ r/R-(1/2)\left(\frac{1}{R/r}\right)\left[1+\left(\frac{1}{R/r}\right)^2\right]\right\}}{\left(r/R-1\right)}. \tag{4}$$

By allowing r = a + R to be substituted in Equation 4 and equating* which in turn is equivalent to Equation 1 results in:

$$K_I/\sigma_0\sqrt{\pi a} = \frac{1+a/R-(1/2)\left(\frac{1}{1+a/R}\right)\left[1+\left(\frac{1}{1+a/R}\right)^2\right]}{a/R}. \tag{5}$$

In Reference 1 the authors examine the biaxially-stressed infinite plate with two cracks located at the hole boundary as shown in Figure 1b. The elastic stresses in the absence of the cracks are given by:[5]

$$\sigma(r) = \sigma_0[1+(R/r)^2]; \tag{6}$$

the mean stress over the crack length a is

$$\sigma_m = \frac{\sigma_0(a/R+2)}{(a/R+1)}; \tag{7}$$

and hence, proceeding as before, the normalized stress intensity factor is

$$K_I/\sigma_0\sqrt{\pi a} = \frac{2+a/R}{1+a/R}. \tag{8}$$

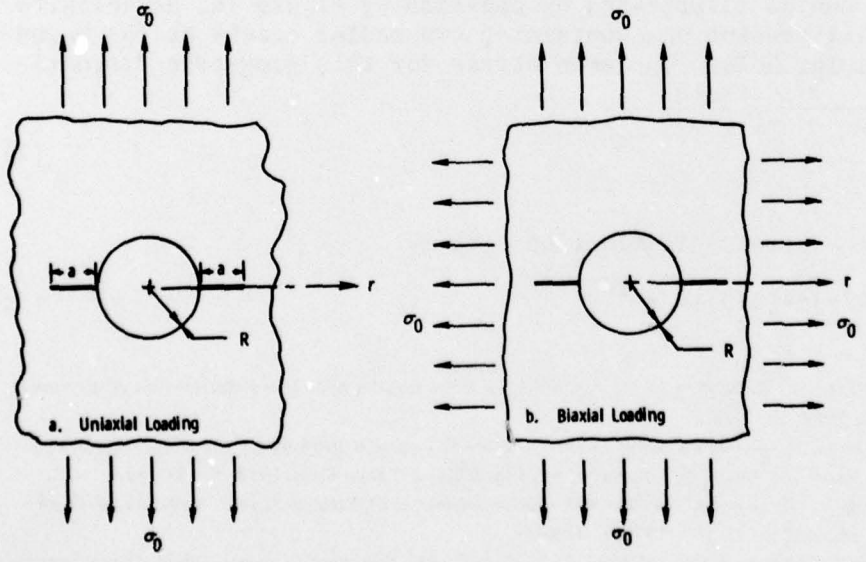

Figure 1. Infinite plate containing radial cracks at the boundary of an internal circular hole.

*The plane stress condition is considered here.

To determine the accuracy of these solutions the normalized stress intensity factor resulting from Equations 5 and 8 are compared to that obtained by Bowie,[6] who solved the same cases by the more exact method of conformal mapping. Such a comparison, showing percent differences for values of a/R from 0 to ∞, are shown in Table 1.

It is seen from the results of Table 1 that for both cases at short crack lengths, a/R = 0, the error is -12%; and as a/R increases the error becomes increasingly positive up to a maximum and then reduces to zero when a/R = ∞. Compensation for an edge crack when a/R is small could be provided, since it is known[7] that for such a configuration normalized stress intensity factor approaches 1.12. This will however increase the overestimate at larger crack ratios. Nevertheless, the method provided by Williams and Isherwood[1] appears to provide estimates of stress intensity factors within engineering accuracy, i.e., ±20%.

In Reference 1 the authors solve several other problems of interest, such as the determination of stress intensity factors for an edge crack in a finite width plate due to bending, an eccentrically-loaded plate with unequal cracks, single-edge-notched, center-notched, double-edge-notched plates, and an eccentric center crack, as well as a radial crack at the bore of rotating disk. Further details of such analyses can be obtained from Reference 1.

The method utilized in Reference 2 will now be demonstrated. Consider Figure 2a, a uniaxially stressed infinite plate with two radial cracks at the boundary of the hole. The stress intensity factor associated with this figure is approximately equivalent to that shown in Figure 2b. The stress distribution $\sigma_{yy}(x,0)$ in an uncracked plate with a hole of radius R is determined at the location of the cracks for the applied loading in question. The crack of length 2a, as shown in

Table 1. COMPARISON OF APPROXIMATE RESULTS TO MORE EXACT DATA FOR AN INFINITE PLATE CONTAINING RADIAL CRACKS

$K_I/\sigma_0\sqrt{\pi a}$

	Two Radial Cracks							
	Uniaxial Stress					Biaxial Stress		
a/R	Ref. 6	Eq. 5	Diff., %	Eq. 11	Diff., %	Ref. 6	Eq. 8	Diff., %*
0	3.39	3.00	-12	2.70	-10	2.26	2.0	-12
0.10	2.73	2.70	-1	2.37	-13	1.98	1.91	-4
.20	2.41	2.47	+2	2.13	-12	1.83	1.83	0
.30	2.15	2.29	+7	1.96	-9	1.70	1.77	+4
.40	1.96	2.15	+10	1.82	-7	1.61	1.71	+6
.50	1.83	2.04	+11	1.72	-6	1.57	1.67	+6
.60	1.71	1.94	+13	1.64	-4	1.52	1.63	+7
.80	1.58	1.80	+14	1.51	-4	1.43	1.56	+9
1.00	1.45	1.69	+17	1.43	-1	1.38	1.50	+9
1.5	1.29	1.51	+17	1.28	-1	1.26	1.40	+11
2.0	1.21	1.41	+17	1.23	+2	1.20	1.33	+11
3.0	1.14	1.29	+13	1.16	+2	1.13	1.25	+11
5.0	1.07	1.18	+10	1.10	+3	1.06	1.17	+10
10.0	1.03	1.10	+7	1.05	+2	1.03	1.09	+6
∞	1.00	1.00	0	1.00	0	1.00	1.00	0

6. BOWIE, O. L. *Analysis of an Infinite Plate Containing Radial Cracks Originating at the Boundary of an Internal Circular Hole.* J. Math. and Phys., v. XXXV, no. 11, 1956, p. 60-71.
7. PARIS, P. C., and SIH, G. C. *Stress Analysis of Cracks.* Fracture Toughness Testing and Its Applications, ASTM STP 381, 1970, p. 30-81.

Figure 2b is pressurized with a symmetric pressure distribution of stress $\sigma_{yy}(x,0)$. The stress intensity factor for through cracks pressurized by this stress distribution of $\sigma_{yy}(x,0)$ is then derived by using the proper Green's function solution for the crack, such as Equation 9, for two symmetric through cracks:[2]

$$K_I\sqrt{\pi(a+R)} = \left[\int_{-a-R}^{-R} \sigma_{yy}(x,0) \sqrt{\frac{a+R+x}{a+R-x}}\, d_x + \int_{R}^{a+R} \sigma_{yy}(x,0) \sqrt{\frac{a+R+x}{a+R-x}}\, d_x \right], \tag{9}$$

where $\sigma_{yy}(x,0)$ obtained from Equation 3 is

$$\sigma_{yy}(x,0) = \sigma_0 \left[1+(1/2)\left(\frac{R}{x}\right)^2+(3/2)\left(\frac{R}{x}\right)^4 \right]. \tag{10}$$

Substitution of σ_{yy} into Equation 9 and integrating between limits gives:

$$K_I/\sigma\sqrt{\pi a} = \sqrt{1+\frac{1}{a/R}} \left[1-(2/\pi)\left\{ \sin^{-1}\left(\frac{1}{1+a/R}\right) - \left(\frac{1}{1+a/R}\right)\left[1+\left(\frac{1}{1+a/R}\right)^2\right] \sqrt{1-\left(\frac{1}{1+a/R}\right)^2} \right\} \right]. \tag{11}$$

Results from Equation 11 are also shown in Table 1 along with the more exact data of Bowie[6] for comparison. It is apparent that Equation 11 differs from those of Reference 6 by -13% at small a/R values, to +3% at larger ratios.

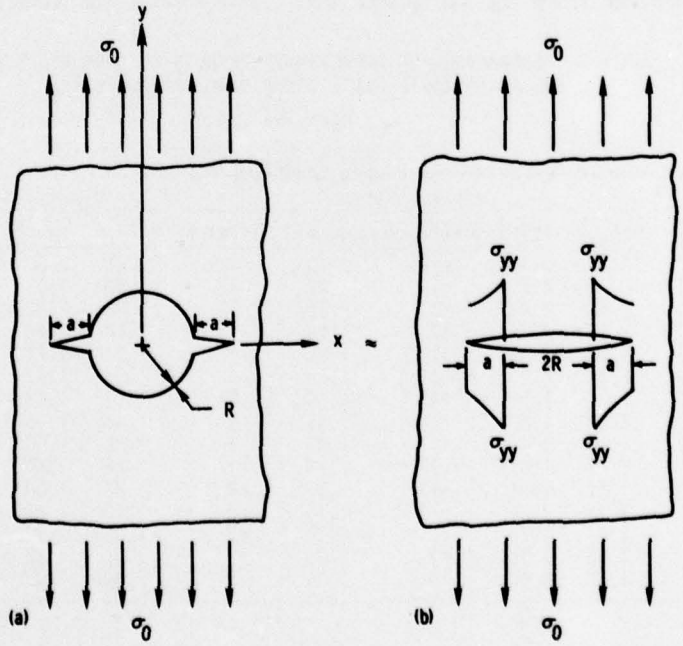

Figure 2. Idealization of a double crack emanating from a hole in a plate.

In the development of this method the crack is assumed to be absent and residual surface tractions on the crack surfaces are eliminated. However, in deriving Equation 5 the *mean* stress arising because of the hole is applied to only *one* radial crack, whereas in arriving at Equation 11 the stress due to the hole is integrated across both crack locations. (Reference 3 allows one to convert from one radial crack to two radial cracks at the hole boundary by the following relationship:

$$K\Big|_{\substack{\text{one}\\\text{crack}}} = \sqrt{(1+a/2R)/1+a/R}\;\; K\Big|_{\substack{\text{two}\\\text{cracks}}} .)$$

Thus, the method of Kobayashi[2] and Shah,[3] although more difficult to apply, is more realistic than that of Williams and Isherwood.[1] Nevertheless, both approaches will provide sufficient accuracy for engineering applications.

The approach suggested by Cartwright[4] and adapted by Baratta[8] will now be outlined. The procedure is one of applying the appropriate stress, associated with the defect discontinuity, to the crack tip for the known limiting cases of stress intensity and utilizing an interpolation scheme between limits to determine intermediate values. It was shown by the preceding illustrative problems how the stress intensity could be approximated by applying to the crack faces the stresses that would normally exist on the plane of the crack, if the crack was absent. However, in the analysis to follow, rather than apply the stress distribution to the crack face, only the stress caused by the defect discontinuity will be applied to the crack tip.

To demonstrate the details of the procedure and evaluate the validity of the approach, it will be applied to a problem already solved by more accurate means. Consider a crack in a region of extreme stress concentration, such as a single radial crack originating from a circular hole in an infinite plate subjected to uniaxial uniform tension at infinity as shown in Figure 3a. This problem, previously used as an example, will be used to evaluate the following approach.

We initially consider the crack length a to be very small compared to the hole radius R. Since the hole radius is very large compared to the crack length we can consider it to be at an edge of a semi-infinite plate, as shown by the equivalent system in Figure 3b, but with a stress distribution $\sigma_\theta(r)$ that arises because of the hole. The normalized stress intensity ratio for an edge crack in a semi-infinite plate stressed in tension at infinity given by Paris and Sih[7] is $K_I/\sigma_0\sqrt{\pi a} = 1.12$, where σ_0 is the remotely applied uniform tensile stress. At the opposite extreme, when the crack length is very large compared to the hole radius, i.e., $a/R \to \infty$, the normalized stress intensity ratio $K_I/\sigma\sqrt{\pi a} = 0.707$, from Reference 6. It appears that this ratio is dependent upon some function of a/R which has limits of 1.12 when a/R = 0 and 0.707 when $a/R \to \infty$. Thus, intermediate values of the normalized stress intensity ratio can be approximated by choosing a function which is well behaved between the above stated limits. The function arbitrarily chosen for this problem as well as those to follow is of the form:

8. BARATTA, F. I. *Stress Intensity Factor Estimates of a Peripherally-Cracked Spherical Void and a Hemispherical Surface Pit.* J. Am. Ceram. Soc., v. 61, no. 11, 1978, p. 490-493; also Army Materials and Mechanics Research Center, AMMRC TR 78-5, March 1978.

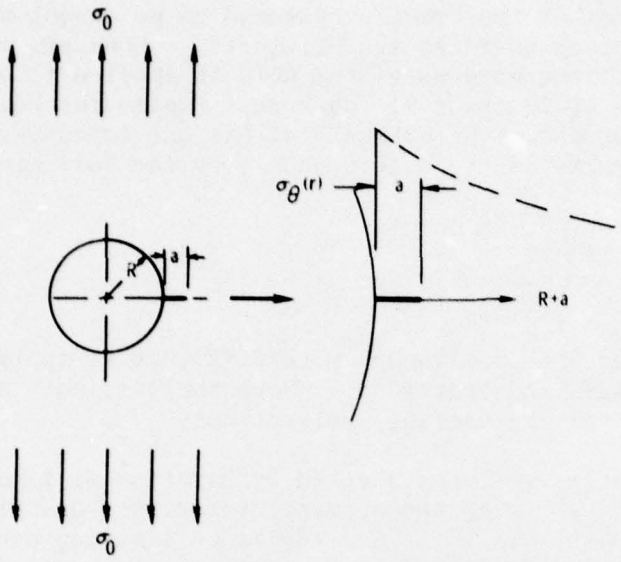

a. Cracked Circular Hole b. Equivalent Cracked Circular Hole

Figure 3. Circular hole with a single radial crack.

$$f(a/R) = Q - M(\tan^{-1}a/R)^m. \tag{12}$$

Thus, for a circular hole with one radial crack the normalized stress intensity ratio is:

$$K_I/\sigma(r)\sqrt{\pi a} = f(a/R) = Q\text{-}M(\tan^{-1}a/R)^m \tag{13}$$

where $\sigma_\theta(r)$ is the stress distribution caused by the circular hole, provided by Timoshenko and Goodier[5] which is Equation 3 in this paper. Substitution of Equation 3 into Equation 13 and transforming the coordinate axis r by R + a, gives

$$K_I/\sigma_0\sqrt{\pi a} = \left[Q\text{-}M(\tan^{-1}a/R)^m \right] \left[1+(1/2)\left(\frac{1}{a/R+1}\right)^2+(3/2)\left(\frac{1}{1+a/R}\right)^4 \right]. \tag{14}$$

Equation 14 represents the estimated normalized stress intensity ratio $K_I/\sigma\sqrt{\pi a}$ for a radial crack of length a emanating from a circular hole of radius R. The particular constants which appear in this equation are readily determined by knowing Q = 1.12 when a/R = 0; M and m are found by allowing f(a/R) = 0.707 when a/R = ∞ and f(a/R) = 0.94 when a/R = 3.0 (taken from Reference 6). With f(a/R) = 0.94, the error span on the function would be minimized throughout the total range of a/R. Thus, Q = 1.12; M was found to be 0.119 and m equals 2.748.

Equation 14 was then utilized to obtain $K/\sigma\sqrt{\pi a}$ as a function of a/R from 0 to ∞. It is seen that these results, shown in Table 2, are within ±6% when compared to the more accurate data of Reference 6. Although the results of this procedure are approximate, it is believed that the errors involved when applied to other analogous problems will be of similar magnitude as those given in the table. Thus, a similar approach is used to solve these problems of interest.

Application of the above technique will be demonstrated by providing estimates of stress intensity factors for a spherical void with a circumferential crack at its equator in an infinite body under uniaxial tensile stress, as shown in Figure 4. Also included is a circumferentially-cracked hemispherical pit at a free surface of a semi-infinite body also stressed by uniaxial tension, shown in Figure 5. Since these types of defects occur in both metallic and ceramic[8] systems such solutions are of interest.

Goodier[9] provided the stress distribution for a spherical defect in an infinite medium stressed in tension. Because of the defect, three stresses are developed, which are indicated

Table 2. COMPARISON OF APPROXIMATE TO EXACT STRESS INTENSITY RESULTS FOR A CIRCULAR HOLE WITH RADIAL CRACK

	$K_I/\sigma\sqrt{\pi L}$		
a/R	From Eq. 14	Ref. 6	Diff., %
0	3.36	3.39	-1
0.1	2.73	2.73	0
.2	2.32	2.30	+1
.3	2.04	2.04	0
.4	1.83	1.86	-2
.5	1.69	1.73	-2
.6	1.56	1.64	-5
.8	1.40	1.47	-5
1.0	1.29	1.37	-6
1.5	1.13	1.18	-4
2.0	1.03	1.06	-3
3.0	0.94	0.94	0
5.0	0.86	0.81	+6
10.0	0.78	0.75	+4
∞	0.708	0.707	0

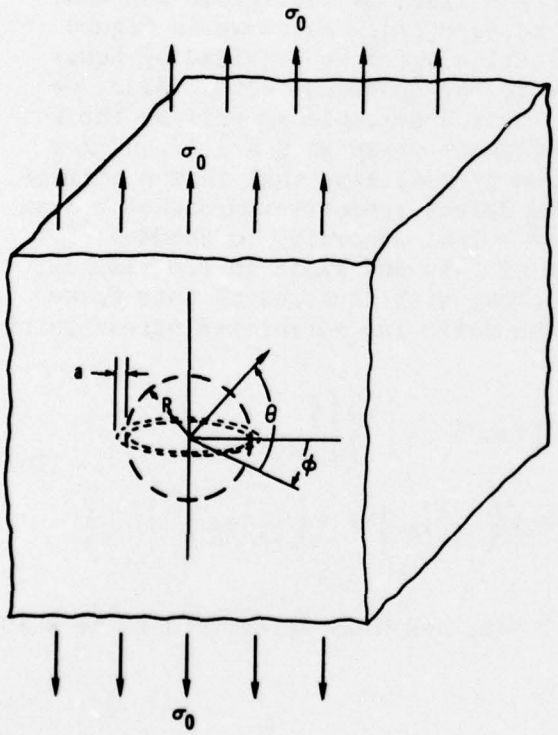

Figure 4. A spherical void with a circumferential crack at its equator.

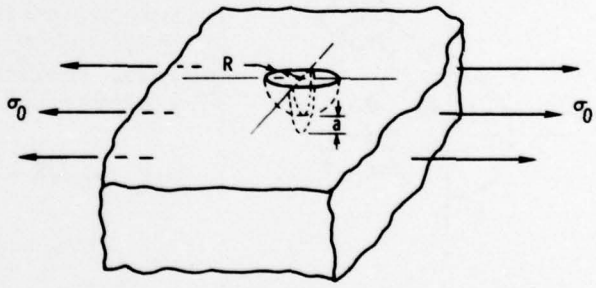

Figure 5. A hemispherical surface pit with a circumferential crack at its semi-equator.

9. GOODIER, J. N. *Concentration of Stress Around Spherical and Cylindrical Inclusions and Flaws.* Trans. ASME, v. 55, 1933, p. 39-44.

schematically in Figure 6. They are: a radial stress σ_r acting normal to the interface, a stress σ_θ acting in a tangential direction to a meridian (the north-south pole axis of the sphere is considered aligned with the axis of the applied stress), and another tangential stress σ_ϕ normal to both σ_r and σ_θ. In the following analysis, the maximum tensile stress is assumed to cause crack initiation.

It is indicated in Reference 9 that the maximum tensile stress for a spherical void occurs when $\theta = 0$, resulting in a "hoop stress" σ_θ which girdles the equator. It is expected that this tensile stress, if large enough, can initiate an axisymmetric crack and extend it in the radial direction as envisioned in Figure 4. The stress distribution when $\theta = 0$ is given in the following equation:

$$\sigma_\theta(r) = \sigma_0 \left\{ \left[\frac{1}{2(7-5\nu)} \right] \left[(4-5\nu) \left(\frac{R}{r} \right)^3 + 9 \left(\frac{R}{r} \right)^5 \right] + 1 \right\}, \tag{15}$$

where ν is Poisson's ratio of the material and r is the radial distance from the center of the spherical void ($r \geq R$).

To obtain an approximation for the stress intensity factor associated with Figure 4, we again initially assume that the crack length a is small compared to the sphere radius R. Also as before, we further assume that when the crack is small, the influence of the spherical void on the crack is negligible and thus can be considered as an edge crack as shown in Figure 3b. Now the stress distribution $\sigma_\theta(r)$ is provided by Equation 15, which is due to the spherical void. Also, we assume that Equation 12 is applicable as well as the constants (except M) previously given as Q = 1.12 and m = 2.748. M is determined by realizing that in the extreme limit when $a/R \to \infty$ the defect geometry approaches a disk crack and thus $K_I/\sigma\sqrt{\pi a} \to 2/\pi$, according to Sneddon.[10] Therefore, making use of this end limit in Equation 12, which is substituted along with Equation 15 into Equation 13, results in the following normalized stress intensity expression:

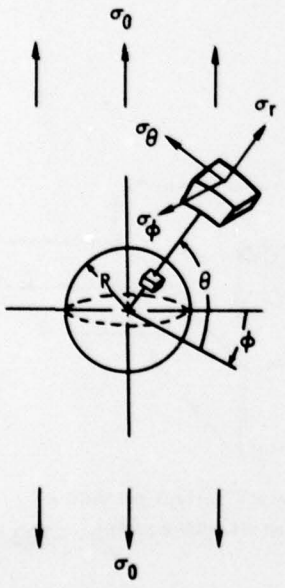

Figure 6. Coordinate system to describe the stress state around a spherical void.

$$K_I/\sigma_0\sqrt{\pi a} = \left[Q - M \left(\tan^{-1} a/R \right)^m \right] \left\{ \left[\frac{1}{2(7-5\nu)} \right] \left[(4-5\nu) \left(\frac{1}{1+a/R} \right)^3 + 9 \left(\frac{1}{1+a/R} \right)^5 \right] + 1 \right\} \tag{16}$$

where Q = 1.12, m = 2.748, and M is determined to be 0.101.

10. SNEDDON, I. N. *The Distribution of Stress in the Neighborhood of a Crack in an Elastic Solid.* Proc. Roy. Soc. London, v. A-187, 1946.

The resulting calculations using Equation 16, which represents the normalized stress intensity ratio for a spherical void cracked at its equator and stressed by uniform uniaxial tension at infinity, are shown in Table 3 as a function of a/R from 0 to ∞ and for $\nu = 0.25$ and 0.30.

The final case considered is a hemispherical pit at a free surface of a semi-infinite body with a crack initiated at the semi-equator of the pit and extended radially by a uniaxial uniform tensile stress as shown in Figure 5. As outlined previously, we initially assume that a is very small compared to R. As before, we further assume that when the crack is small, the influence of the hemispherical pit on the crack is negligible and thus can be considered an edge crack as shown in Figure 3b, with the stress distribution $\sigma_\theta(r)$ caused by the surface pit discontinuity. Again as before, we utilize Equation 13, with Q = 1.12 and m = 2.748, but determine M from the end limit when $a/R \to \infty$. Smith and Alavi[11] give the variation of $K_I/\sigma\sqrt{\pi a}$ around the semicircular crack boundary and indicate that the maximum value occurs at the junction of the crack with the free surface and is $1.21 \times 2/\pi$. This results in M = 0.140.

The stress distribution $\sigma_\theta(r)$ is provided by Eubanks,[12] who determined the variation of the circumferential stress along the axis of symmetry as a function of r at the base of the pit. Equation 12, including the constants previously given, i.e., Q = 1.12, m = 2.748, and M = 0.140, and the normalized stress distribution $\sigma_\theta(r)/\sigma_0$ given in tabular form, will provide the normalized stress intensity ratio for a peripherally-cracked hemispherical surface pit with $\nu = 0.25$. Such results, including $\sigma_\theta(r)/\sigma_0$, are given in Table 4 as a function of a/R from 0 to ∞.

The application of Equation 14 and Tables 3 and 4 has certain restrictions resulting from the implied assumptions used in References 9 and 12 when determining the appropriate stress distribution. These restrictions are:

The material is isotropic and homogenous.

The defect, which includes the crack, is very large compared to the grain size of the crystalline aggregate.

Table 3. STRESS INTENSITY RATIO FOR A PERIPHERALLY-CRACKED SPHERICAL VOID

	$K_I/\sigma_0\sqrt{\pi a}$	
a/R \ ν	0.25	0.30
0	2.26	2.30
0.15	1.73	1.75
0.35	1.41	1.41
0.55	1.26	1.26
1.00	1.10	1.08
2.00	0.94	0.93
3.00	.86	.86
5.00	.79	.79
10.00	.72	.72
∞	.64	.64

Table 4. NORMALIZED STRESS INTENSITY RATIO FOR A PERIPHERALLY-CRACKED HEMISPHERICAL SURFACE PIT, WITH $\nu = 0.25$

a/R	$\sigma_\theta(r)/\sigma_0$	$K_I/\sigma\sqrt{\pi a}$
0	1.23	2.50
0.15	1.63	1.82
0.35	1.29	1.44
0.55	1.15	1.27
1.00	1.04	1.11
2.00	1.00	0.99
3.00	1.00	.93
5.00	1.00	.88
10.00	1.00	.83
∞	1.00	.77

11. SMITH, F. W., and ALAVI, M. J. *Stress Intensity Factors for a Part-Through Circular Surface Flaw.* Proc. 1st Intl. Conf. on Pressure Vessel Tech., Delvt, Holland, 1969.

12. EUBANKS, R. A. *Stress Concentration Due to Hemispherical Pit at a Free Surface.* J. Appl. Mech., v. 21, 1954, p. 57-62.

The tip of the crack, which surrounds the spherical void, can be no closer than 2R + 2a to a body boundary.

The tip of a crack, which surrounds a hemispherical pit at a free surface, can be no closer than R + a away from any other body boundary.

Since there are no other available solutions to effect a comparison of the three-dimensional cases given above their accuracy can not be definitively ascertained. However, the author[8] of this technique claims that engineering accuracy is preserved.

SUMMARY

It is seen that the method used by Williams and Isherwood[1] as applied to two radial cracks emanating from a circular hole stressed by uniaxial tension resulted in a range of error of -12% to +17%. For this particular class of problems the approach does not allow differentiation between the one-crack case and two-crack case. This method should be restricted in application to those problems where only one crack is present.

The more complex method of Kobayashi[2] and Shah[3] will allow such flexibility and is more accurate, i.e., the error ranged from -13% to +3% for the same problem. However, for the two-crack biaxial stress case the range of error, when compared to Bowie's results[6] was -12% to +11%. Nevertheless, both methods will provide results that can be adapted for engineering applications.

The approach suggested by Cartwright[4] and adapted by Baratta[8] is even easier to apply but one must know the end limit to obtain an interpolation relationship. The resulting accuracy is not definitively known for the three-dimensional cases solved but it is believed that it should be well within acceptable standards for engineering applications.